Chinese Journal of Polymer Science Vol. 34, No. 7, (2016), 873–888

Chinese Journal of Polymer Science
© Chinese Chemical Society
Institute of Chemistry, CAS
Springer-Verlag Berlin Heidelberg 2016

Synthesis of Branched Poly(butylene succinate): Structure Properties Relationship*

Marie Vandesteene[d], Nicolas Jacquel[c], René Saint-Loup[c], Nadège Boucard[d], Christian Carrot[b], Alain Rousseau[a] and Françoise Fenouillot[a**]

[a] *Unive Lyon, INSA-Lyon, Ingénierie des Matériaux Polymères, IMP, UMR5223, F-69621, Villeurbanne, France*
[b] *Univ Lyon, Université Jean Monnet, Ingénierie des Matériaux Polymères, IMP, UMR5223, F-42023 Saint-Etienne, France*
[c] *Roquette Frères, Polymer Chemistry Department, F-62136 Lestrem, France*
[d] *MBD Texinov, F-38110 Saint-Didier-de-la-Tour, France*

Abstract A series of branched poly(butylene succinate) (PBS) were synthesized with several branching agents namely trimethylol propane (TMP), malic acid, trimesic acid, citric acid and glycerol propoxylate. The structure of the branched polymers was analyzed by SEC and ^{1}H-NMR. The effect of branching agent structure on crystallization was also investigated and played a significant role. Isothermal studies showed that glycerol propoxylate could act as a nucleating agent. By contrast high content of TMP disturbed the regularity of the chain and hindered the crystallization of PBS. From the non-isothermal kinetic study, it was found that glycerol propoxylate increased noticeably the crystallization rate due to the flexible structure of the branching agent. A secondary nucleation was observed with glycerol propoxylate attributed to the crystallization of amorphous fraction included between crystallites formed at the primary crystallization. Chain topology was obtained through rheological investigations and the synthesized polymers showed a typical behavior of a mixture of linear and randomly branched PBS. The incorporation of branches improved the processability of PBS for film blowing application and the modulus and the stress at break of the resulting film were significantly increased.

Keywords: Poly(butylene succinate); Branching; Crystallization; Properties.

Electronic Supplementary Material Supplementary material is available in the online version of this article at http://dx.doi.org/10.1007/s10118-016-1805-5.

INTRODUCTION

Recently with the growing concerns on accumulation of plastic waste there is a desire to use biodegradable polymers for applications in the field of food packaging, agriculture or disposable items. Among biodegradable polymers, poly(butylene succinate) (PBS) possesses a high melting temperature but also mechanical properties close to the ones of low density polyethylene. However, like most biodegradable polymers, PBS suffers from low melt strength and needs to be modified to facilitate its use for application such as film blowing[1]. Chain branching during the synthesis appeared to be one of the promising solutions to improve PBS processability. A PBS bearing long chain branches has been commercialized in the 90s to ease its processing in applications such as blow molding or foamed sheet[2].

* This work was financially supported by the company MBD Texinov (France), the company Roquette Frères (France) and the ANRT. The work was done within the framework of the collaborative project Agroboost funded by BPI France, and also Rhone-Alpes Region, Rhone-Alpes FEDER and the Basse Normandie Regional Council.
** Corresponding author: Françoise Fenouillot, E-mail: francoise.fenouillot@insa-lyon.fr
Received January 17, 2016; Revised February 22, 2016; Accepted February 23, 2016
doi: 10.1007/s10118-016-1805-5

Up to date several strategies have been reported in literature to obtain various types of branched PBS. Generally polyols were used as comonomers with succinic acid and 1,4-butanediol in the polymerization reactor. These polyols include glycerol[3] (functionality $f = 3$), trimethylolpropane[4] ($f = 3$), 1,2,4-butanetriol ($f = 3$)[5], castor oil ($f = 2.6$) or polyglycerol ($f \approx 7$)[6]. Branched poly(butylene adipate)s were also synthetized using pentaerythritol ($f = 4$) or glycerol[7]. A multifunctional acid, trimesic acid ($f = 3$) may also be used[8].

Unsaturated groups were introduced in the main chain *via* copolymerization with maleic acid[9, 10]. The unsaturated groups were then subjected to reaction with benzoyl peroxide to form branch knots. Branched PBS could also be achieved *via* radical interchain transfer using an electron beam in the presence of polyfunctional monomers bearing double bonds[11]. Finally linear PBS was also modified through reactive melt mixing with chain extender having multi epoxy-groups[12].

In the second approach, short preformed pending chains could be simply inserted in the polymer chains. Such copolymers were made of succinic acid, butanediol and 1,2-octanediol[13], 1,2-butanediol or 1,2-decanediol[14].

As a general trend, short-chain branches decrease crystallization rate and melt viscosity, limiting its applications. By contrast, long branches enhance melt viscosity, shear thinning and extension thickening which is desirable for processing. Moreover, the presence of a branching agent could modulate the biodegradability of the polymer[8, 15].

As reported by McKee *et al*. in their review, the relationship between the structure and the properties of branched polyesters is complex and thus more systematic testing is needed to have a better understanding of all phenomena[15]. In the present study, PBS was branched with the help of five different types of branching agents: trimethylolpropane, malic acid, trimesic acid, glycerol propoxylate and citric acid. The effect of branching agents on the synthesis, crystallization behavior, rheological and tensile properties was studied in detail and correlated to their branching structure.

EXPERIMENTAL

Materials

Petrochemicals based succinic acid (SA, 99.72%) and 1,4-butanediol (BDO, 99.3%) were respectively purchased from Gadiv Petrochemical Ind. (Haifa, Israel) and Sigma-Aldrich (France). Titanium(IV) *n*-butoxide (99%, Acros Organics) was used as a catalyst. Branching agents used in this study were: malic acid (99%, Sigma Aldrich), trimethylol propane (also known as 1,1,1-tris(hydroxymethyl)propane) (≥ 98.0%, Aldrich), trimesic acid (also known as benzene-1,3,5-tricarboxylic acid) (95%, Aldrich), citric acid (also known as 2-hydroxypropane-1,2,3-tricarboxylic acid) (99%, Aldrich) and glycerol propoxylate (Aldrich, M_n = 266 g/mol) also sold under the trade name Voranol 450 by Dow Chemicals (M_w = 450 g/mol). All these chemicals were used as received without further purification. Figure 1 and Table 1 summarize their structure and properties, respectively.

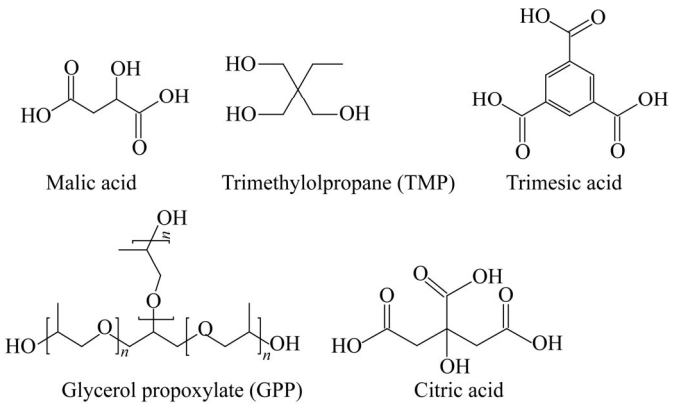

Fig. 1 Multi-functional branching agents used in the study

Table 1. Properties of multi-functional branching agents

	Malic acid	Trimethylolpropane (TMP)	Trimesic acid	Glycerol propoxylate (GPP)	Citric acid
M (g/mol)	134	134	210	266	192
T_m (°C)	131	58	374	–	153
b_p (°C)	306 [a]	289	–	–	175

[a] Starts to decompose at 150 °C

Synthesis of Branched PBS

The procedure used for the synthesis of the polymer is similar to the one described elsewhere[16]. 400 mg of titanium per kg of PBS polymer was used. To avoid any gelation of the polymer in the pilot reactor, the addition of trifunctional monomers was limited in order to obtain a branching ratio lower than 1%. A particular attention was taken in order to keep the hydroxyl/acid molar ratio constant to r = 1.05, thus avoiding the influence of this ratio on the polycondensation rate.

Solution Viscosity

The reduced viscosity, η_{red} of the polymers was determined with an automated Ubbelohde capillary at 25 °C. Polymer samples were dissolved during 15 min up to 25 min at room temperature in a mixture of phenol/ortho-dichlorobenzene (50:50 wt%, Aldrich France) at the concentration c = 5 g/L. Then reduced viscosity was calculated according to Eq. (1). t_0 and t_s respectively refer to neat solvent and polymer-solvent solutions flow times.

$$\eta_{red} = \frac{t_s - t_0}{t_0 \times c} \tag{1}$$

Nuclear Magnetic Resonance Spectroscopy ^{1}H-NMR

The ^{1}H-NMR analysis of branched PBS was carried out at 25 °C on a 400 MHz Bruker liquid state NMR spectrometer equipped with a QNP/BBFO+ probe. The polymer samples were dissolved in deuterated chloroform for analysis.

The hydroxyl and carboxylic end group contents were determined by ^{1}H-NMR. Two pellets of PBS (about 0.020 g) were dissolved in $CDCl_3$ (5 mL). Then trifluoroacetic anhydride (TFAA) (1 mL) was added to the solution. After 30 min, ^{1}H-NMR analysis was performed. Integration of the $\delta = -2.9$ [t, 2H] peak for the PBS-trifluoroacetic anhydride allowed quantification of the acid end-groups and integration of the $\delta = -4.4$ [t, 2H] for the trifluoroacetate of PBS allowed quantification of the hydroxyl end-groups.

Size Exclusion Chromatography (SEC)

Polymer molar mass has been assessed by size exclusion chromatography in 1,1,1,3,3,3-hexafluoro-2-propanol (HFIP). 1 g/L samples were eluted at the flow rate of 0.75 mL/min. Signals were then detected by using an UV detector (Agilent-UV-272) combinated with a RI detector (Agilent-RI-1100). The average molar masses M_n and M_w were determined with a calibration method using polymethyl methacrylate (PMMA) standards.

Thermal Properties

The thermal properties of the PBS have been measured on a TA Instrument Q10 differential scanning calorimeter. The polymer sample was first heated from −80 °C to 150 °C (10 K/min), the temperature was then held for 2 min before cooling to −80 °C (10 K/min). Temperature was also held for 2 min before a second heating in the same conditions as in the first step. The glass transition of the polymer was taken at midpoint during the second heating. The melting temperature was taken at peak minimum during the second heating scan. The melting enthalpy was calculated from the integration of this melting peak and cold-crystallization peak. The crystallinity, χ_c, of PBS was calculated according to Eq. (2).

$$\chi_c(\%) = \frac{\Delta H_m - \Delta H_{cc}}{\Delta H^0_{PBS}} \tag{2}$$

ΔH_m is the melting enthalpy of the sample (J/g), ΔH_{cc} is the enthalpy of the small cold-crystallization peak typically observed around 90 °C and ΔH^0_{PBS} is the melting enthalpy of the fully crystalline PBS which is assumed to be 210 J/g[17]. The crystallization temperature was measured at peak maximum during the cooling scan.

Non-isothermal and Isothermal Crystallization Kinetic Study

The procedure described above was applied for non-isothermal crystallization kinetics studies except that the cooling rate before the second heating ramp was set at 10, 20, 30 and 40 K/min.

Isothermal crystallizations were performed at temperatures ranging from 74 °C up to 90 °C. Samples were first heated to 150 °C and hold at this temperature for 3 min to erase their thermal history and to remove the existing crystalline phase. The crystallization temperature T_c was then reached rapidly (100 K/min) and maintained for 90 min.

Dynamic Shear Rheology

Melt rheology under oscillatory shear was investigated with an ARES rheometer from Rheometrics. A parallel plate (diameter = 25 mm, gap = 1.2 mm) geometry was selected for frequency sweeps under controlled strain in the linear domain (20%). Angular frequencies were swept from 100 rad/s to 0.05 rad/s, and testing was carried out at 130 °C.

Extrusion Blowing of Thin Films and Tensile Test

PBS films were obtained by extrusion film blowing. Dry polymer pellets (one night at 80 °C under vacuum) were extruded in a Collin Teach-line single screw extruder E20T through a film blowing unit Collin Teach-line BL20T equipped with an annular die (30 mm die diameter and 0.8 mm slot width).

For all films, the temperature profile in the extruder was set at 160 °C and the operating temperature of the die was tuned in order to obtain optimal processing conditions, bubble stability and visual film quality. Tensile tests were performed on normalized H3 dog-bone tensile samples of 4 mm width, with a nominal length of 10 mm and a thickness comprised between 30 μm and 50 μm. All tests were performed at the rate of 50 mm/min on a MTS testing system at room temperature.

RESULTS

The branching ratio, X_B in mol%, has been defined as the number of branches for 100 monomer units. One molecule of the selected branching agent inserts one branch in the PBS chain. As a consequence the branching ratio corresponds approximately to the molar percentage of branching agent relative to the total monomer introduced in the feed. The $CHCl_3$ insoluble gel fraction of branched PBS remained quite constant and comprised between 0.2 wt% and 1.1 wt% (0.2 wt% for linear PBS).

Synthesis and Polymer Molar Mass

The addition of branching agent did not affect much the esterification reaction that proceeded as for a typical synthesis of linear PBS. However since branching has an impact on melt viscosity, its effect is indeed detectable when molar mass increases substantially during the polycondensation stage of the synthesis. As shown in Fig. 2, the higher the quantity of branching agent introduced, the faster the torque C increases during polycondensation. This of course can be explained by the increasing proportion of branches which tends to increase the melt viscosity.

The type of branching agents plays also a role as can be seen in Fig. 3 where torque rise is depicted for 0.22 mol% branching agent in feed. The viscosity increase at different rates is probably related to the rate of incorporation and growth of the branches and to the polymer macromolecular structure. Nevertheless it is difficult to categorize the effects and to propose a consistent explanation for this feature.

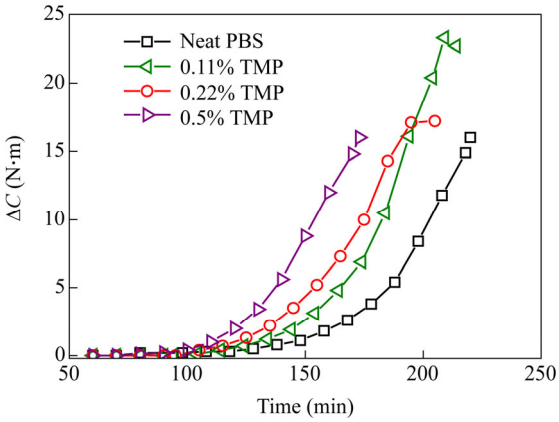

Fig. 2 Torque variation during polycondensation for PBS with various amounts of trimethylolpropane

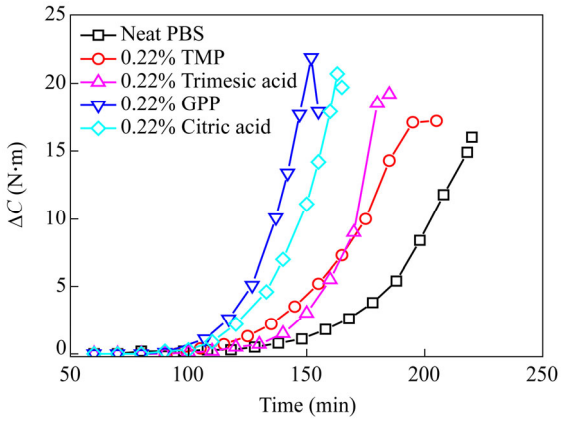

Fig. 3 Torque variation during polycondensation for PBS with 0.22 mol% of different branching agents

From the results given in Table 2 it appears that branching agents were quite well incorporated in the final polymer. However, according to NMR measurements, only half of the malic acid has been incorporated in the chain. Malate was prone to degradation and its deshydratation produced fumarate and maleate moieties as assessed by ^{1}H-NMR measurements (peak at $\delta = 6.24$ for maleate groups and $\delta = 6.84$ for fumarate groups). The maleate and fumarate moieties formed do not lead to branch points.

Table 2. Properties of linear and branched PBS obtained after polymerization

Branching agent		PBS	Trimethylolpropane			Malic acid		Trimesic acid	Glycerol propoxylate	Citric acid
Branching ratio (X_B)	in feed (mol%)	0	0.11	0.22	0.5	0.22	0.5	0.22	0.22	0.22
	in polymer [a] (mol%)	0	0.09	0.2	0.37	0.12	0.3	0.19	0.16	0.14
η_{red} (mL/g)		192	211	212	228	217	211	187	164	181
M_w [b] (10^5 g/mol)		1.081	1.489	1.745	2.214	1.034	1.484	1.667	1.532	1.484
M_n [b] (10^4 g/mol)		5.625	5.69	5.09	3.895	4.31	4.24	4.975	5.16	5.06
PDI [b]		1.9	2.6	3.4	5.7	2.4	3.5	3.3	3	2.9
End-group content [a] (μeq/g)	OH	11	18	30	117	–	–	55	21	35
	COOH	43	70	76	23	–	–	59	67	53
	Total	54	88	106	140			114	88	86
DP_n [c]		427	302	284	243	–	–	255	317	324
M_n [d] (10^5 g/mol)		3.66	2.60	2.43	2.09	–	–	2.19	2.72	2.80
Number of branches per chain [e]		–	0.28	0.57	0.89	–	–	0.49	0.55	0.45

[a] Measured by ^{1}H-NMR; For citric acid, branching agent introduced was estimated by the summation of the integration of citric acid and aconitic acid; [b] Measured by SEC in HFIP with PMMA standards; [c] Calculated with Eq. (3); [d] Calculated with Eq. (4); [e] Calculated with Eq. (5)

Citric acid also degraded by deshydratation of the hydroxyl function into aconitic acid, however, this moiety, incorporated in the chain can still be a branch point compared to malate and fumarate since citric acid has already 3 carboxyl functions accessible.

Although patents report the use of malic acid in PBS[18–20], malic acid has two carboxylic groups and one secondary hydroxy group, the latter being perhaps not very accessible to form branching. PBS branched with

malic acid was not further studied.

As expected molar mass and dispersity index are higher when the amount of branching agent increases. A maximal PDI value of 5.7 was obtained for 0.5 mol% of TMP. Judging from the molar mass distributions given in Fig. 4, one shoulder in the high molar mass region could be observed with 0.5 mol% TMP. This bimodal distribution might be associated with the presence of two different hydrodynamic volumes associated to different topologies.

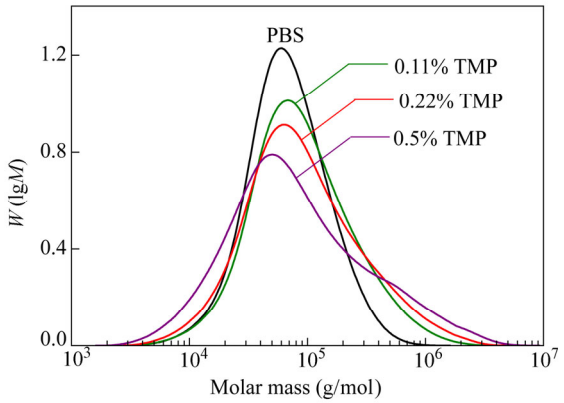

Fig. 4 Molar mass distribution for PBS branched with trimethylolpropane

We already discussed the determination of the molar mass of linear PBS in a previous paper[21]. The determination of molar mass of branched polymers by SEC using a monodetector is not accurate due to the fact the topology greatly affects the hydrodynamic volume. Determination of molar mass has thus been performed using ^{1}H-NMR by determining the mole fractions of terminal (X_T), trifunctional branching (X_B) and linear (X_L) constitutive monomers. DP$_n$ is calculated with Eq. (3).

$$\mathrm{DP}_n = 2 \times \frac{X_T + X_B + X_L}{X_T - X_B} \tag{3}$$

The number average molar mass is calculated using Eq. (4).

$$M_n = \mathrm{DP}_n \, M_0 \tag{4}$$

where $M_0 = M_L \, X_L + M_B \, X_B + M_T \, X_T$ is the average molar mass of the constitutive monomeric mixture. M_L, M_B and M_T are the molar masses of the monomers constitutive units.

The average number of branches per chain is calculated using Eq. (5).

$$\text{Number of branches per chain} = \frac{X_B}{\frac{X_T + X_B}{2}} \tag{5}$$

From the results exposed in Table 2, we can notice that M_w and PDI increase significantly when the amount of TMP increases. This is due to the formation of long branches. On the other hand, M_n decreases because we decided to stop the polymerizations at a stirrer torque that was approximately the same for all synthesis (remind that stirrer torque is related to M_w, not to M_n). This implies that the reaction time and thus conversion were actually shorter for PBS polymerization with branching agents. Indeed we obtained linear chains with lower molar mass because of the lower conversion. This is clearly visible on SEC results. The peak maximum is shifted toward lower value of molar mass and a shoulder appears in the high molar mass region that corresponds to branched chains (Fig. 4). The number of branches per chain is around 0.5 for PBS branched at 0.22% meaning that half of the chains composing the polymer are linear. At 0.5% TMP about 0.9 branches per chains were found. The amount of linear chains might be considerably reduced.

Concerning the carboxylic end group content of the polymer, the introduction of TMP, citric acid, trimesic acid and glycerol propoxylate reduced significantly the amount of carbonyl chain ends giving an advantage against hydrolytic degradation. This can be correlated with the lower reaction time since carboxyl chain ends appear for long reaction time.

Thermal Behavior of Linear and Branched PBS

Thermal properties

The thermal properties of linear and branched PBS are given in Table 3. All samples displayed similar global melting and crystallization behavior with one small cold crystallization peak at 95 °C followed by a single melting peak around 112 °C and one crystallization peak around 63 °C. This behavior is typical of linear high molar mass PBS as found by Jin *et al*. in a study where they varied the molar mass of the polyester[22]. Among samples with branching agents, significant differences are detected when looking at crystallization temperature, T_c. While TMP retards the crystallization to lower temperatures (−1/−3 K), glycerol propoxylate brings the crystallization to higher temperature (+4 K). The commercial branched PBS Bionolle also shows an increase in T_c compared to the linear one[23]. This increase in T_c was also observed by Wang *et al.* with 1,2,4-butanetriol in PBS (+5 K), however the crystallinity showed a marked decrease with increasing content of branching agents[13]. In our study, crystallinity remained stable.

Table 3. Thermal properties of linear and branched PBS

Branching agent	Branching in polymer (mol%)	T_g (°C)	T_m (°C)	T_c (°C)	χ_c (%)	Avrami parameters of PBS crystallized at T =			
						74 °C		90 °C	
						K	n	K	n
PBS	0	–31	112	65	25.6	1.9×10^{-1}	2.2	2.1×10^{-4}	2.4
Trimethylolpropane	0.14	–31	112	65	25.8	1.8×10^{-1}	2.2	3.9×10^{-5}	3.0
	0.20	–31	111	64	25.6	1.9×10^{-1}	2.1	6.4×10^{-5}	2.7
	0.39	–31	111	62	24.7	1.1×10^{-1}	2.2	8.4×10^{-6}	2.9
Trimesic acid	0.21	–31	112	66	25.8	2.8×10^{-1}	2.4	1.5×10^{-4}	2.6
Glycerol propoxylate	0.16	–31	111	69	26.0	11×10^{-1}	2.6	7.4×10^{-4}	2.2
Citric acid	0.22 (in feed)	–31	111	65	25.3	2.3×10^{-1}	2.5	3.9×10^{-5}	2.7

On the other hand, trimesic acid, malic acid and citric acid have no significant impact on the crystallization temperature. TMP was studied in the largest range of concentrations. It appears that both crystallization and melting temperatures decrease for increasing amounts of this branching agent. This behavior is in accordance with observations of Kim *et al*. for PBS containing TMP[4].

To bring further information about crystallization kinetics, isothermal and non-isothermal kinetic studies will be discussed.

Isothermal crystallization

Crystallization kinetics was estimated by fitting experimental data with the Avrami equation[25]. Relative crystallinity $X(t)$ was calculated by dividing the under-curve area of the crystallization exotherm dH_c/dt, at a time t by that of the end of crystallization according to Eq. (6).

$$X(t) = \frac{\int_{t_i}^{t} (\frac{dH_c}{dt}) dt}{\int_{t_i}^{t_f} (\frac{dH_c}{dt}) dt} \tag{6}$$

t_i is the time when crystallization starts and t_f the time when crystallization is completed. All plots will not be exposed herein. From the Avrami theory can be calculated the relative crystallinity $X(t)$ at a given time t using Eq. (7).

$$X(t) = 1 - \exp(-Kt^n) \tag{7}$$

where K is the crystallization rate constant at a fixed temperature and n is the Avrami exponent, which is related to the nucleation mechanism and crystal grown dimensions. In turn, K can be calculated according to Eq. (8).

$$K = \frac{\ln 2}{t_{\frac{1}{2}}^{\,n}} \tag{8}$$

As an example Fig. 5 depicts the relative crystallinity and Avrami plot for PBS branched with glycerol propoxylate.

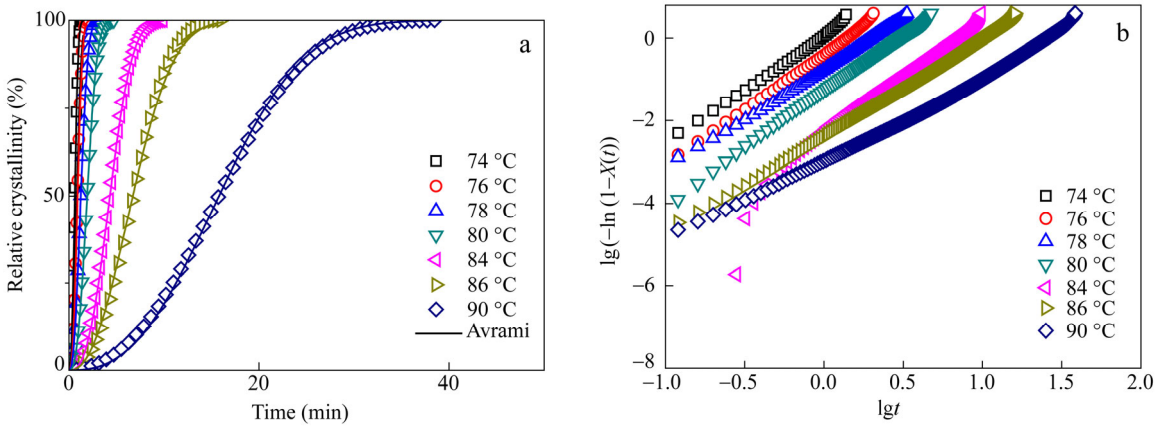

Fig. 5 (a) Relative crystallinity versus crystallization time and (b) avrami plot for PBS branched with 0.22% glycerol propoxylate at different crystallization temperatures
The geometrical points represent experimental data while the continuous lines are the results of theoretical Avrami model.

Avrami parameters extracted from the plots are exposed in Table 3 and the detailed results are given in supporting data Table S1. Based on the slope of the lines of the Avrami plot, the Avrami exponent n is found to range from 2 to 2.7. The values found for n means that the crystallization mechanism is a three-dimensional spherulite growth with heterogeneous nucleation mechanism or a homogeneous nucleation accompanied by two-dimensional growth. The crystallization rate K was found to largely increase with 0.22 mol% of glycerol propoxylate and to decrease with 0.5 mol% of TMP. Values for other branching agents were close to linear PBS. This means on one hand that the crystallization rate is enhanced with branching with glycerol propoxylate. The branch point could act as a nucleating agent. On the other hand a high TMP content might disturb the regularity of the chain and hinder the crystallization of PBS. The half time curves versus temperature are shown in Fig. 6. The minimum of half time is found at 74 °C. Measurements could not be performed at lower isotherm temperatures since cooling from the melt induced a marked pre-crystallization. The results of half time crystallization confirmed the previous results. While trimesic acid and glycerol propoxylate can be classified as crystallization enhancer, TMP is considered to hinder isothermal crystallization.

Non-isothermal crystallization

The non-isothermal crystallization was studied under four different cooling rates. Figure 7 shows the plots of relative crystallinity at 40 K/min cooling rate versus temperature of linear PBS. With increasing the cooling rate the crystallization exotherms became broader and shifted to lower temperatures. This behavior means that at high cooling rates the crystallization onset is delayed and ends also later since the polymer has less time to form crystals[26, 27].

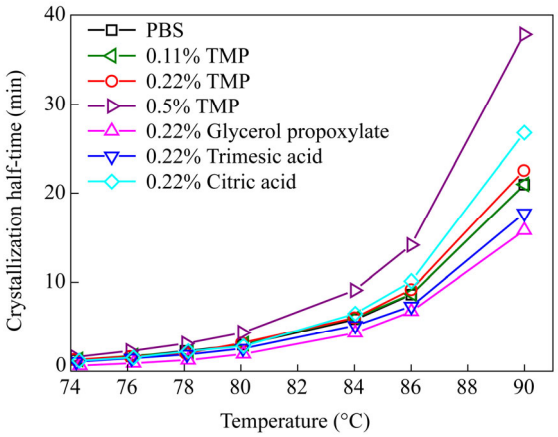

Fig. 6 Crystallization half time versus temperature for linear and branched PBS

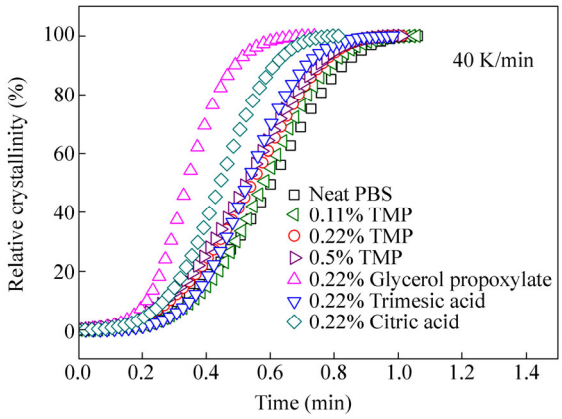

Fig. 7 Plots of relative crystallinity versus time at 40 K/min cooling rate for linear and branched PBS

Relative crystallinity was calculated from the crystallization exotherm as a function of temperature, dH_c/dT, at each cooling rate, as in Eq. (9).

$$X(T)=\frac{\int_{T_i}^{T_{crys}}(\frac{dH_c}{dT})dT}{\int_{T_i}^{T_f}(\frac{dH_c}{dT})dT} \tag{9}$$

T_i is the initial crystallization temperature, T_{crys} is the crystallization temperature at a time t and T_f is the temperature when the crystallization is complete.

The crystallization temperature was then converted to crystallization time according to Eq. (10).

$$t=\frac{(T_0-T_{crys})}{\phi} \tag{10}$$

T_{crys} is the temperature at crystallization time t, T_0 the temperature at the onset of crystallization, ϕ is the cooling rate.

From these results, the crystallization half time $t_{1/2}$ was calculated and its values at different cooling rates are plotted in Fig. 8. The influence of long chain branching is dependent on the branching agent used. However, by contrast with the isothermal study, the crystallization rate was increased with all branching agents compared to linear PBS at cooling rates above 10 K/min.

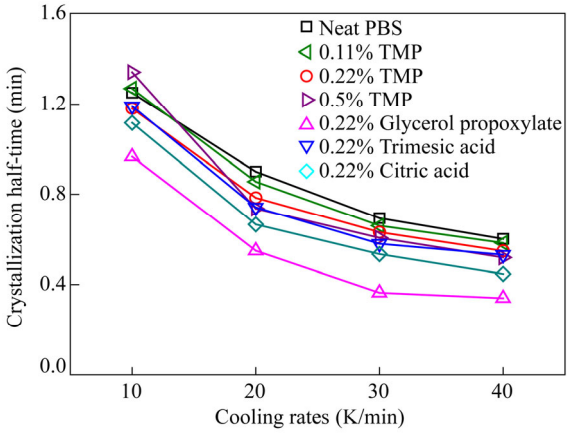

Fig. 8 Crystallization half time versus cooling rate for linear and branched PBS

Jeziorny modified avrami model

Similar to the isothermal analysis, the Avrami equation was adopted to analyze the non-isothermal crystallization (Eq. 11).

$$-X(t) = \exp(-Z_t t^n) \tag{11}$$

$X(t)$ is the relative crystallinity, n the Avrami constant and Z_t the crystallization rate constant. Plots of the double logarithm for PBS and branched PBS with glycerol propoxylate are exposed in Fig. 9 and the kinetic parameters for all samples are given in supporting data (Table S2).

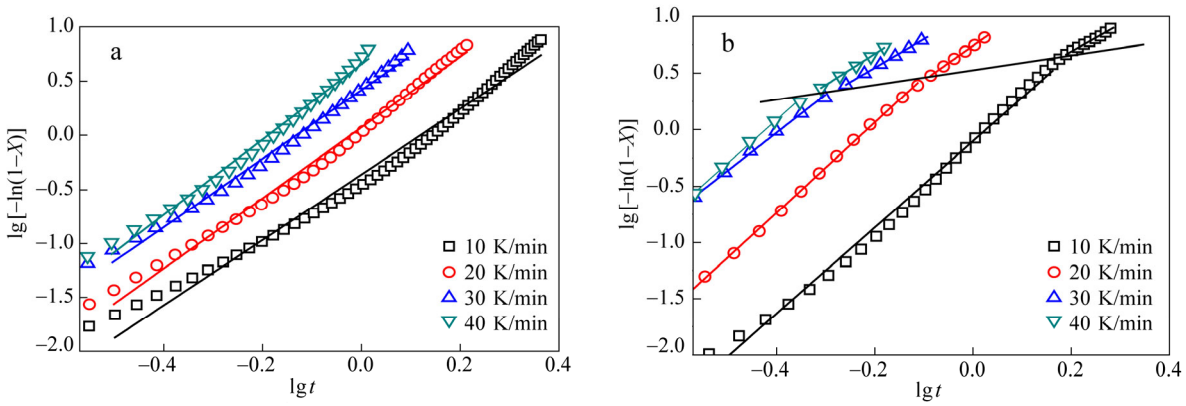

Fig. 9 Avrami plots of (a) PBS and (b) branched PBS with glycerol propoxylate at different cooling rates

One can notice a linear relation for the PBS sample, while the curve of PBS branched with glycerol propoxylate shows a break. The same behavior was observed with trimesic acid but was less marked. This assesses that there are two crystallization regimes governing the crystallization: the first one is the nucleation and growth of crystalline entities and the second one appears when the crystalline entities get a critical size and is attributed to the crystallization of amorphous fraction including between crystallites formed at the primary crystallization.

Considering the temperature change during the non-isothermal process, Jeziorny revised Z_t with the rate of cooling rate ϕ according to Eq. (12)[28].

$$\lg Z_c = \frac{\lg Z_t}{\phi} \tag{12}$$

Z_c values of the primary crystallization of branched PBS with TMP are close to the ones of PBS while $t_{1/2}$ decreases. It can be concluded that TMP acts on crystal growth rate without having a nucleating effect. Nevertheless for glycerol propoxylate, citric acid and trimesic acid the values of Z_c increased and $t_{1/2}$ decreased as the cooling rate increased, which meant an increase of crystallization rate. For a given cooling rate, Z_c for 0.22% glycerol propoxylate was higher than that for trimesic acid and citric acid and $t_{1/2}$ was lower, signifying that PBS with 0.22% glycerol propoxylate had a faster crystallization.

The presence of a secondary crystallization with glycerol propoxylate and the improvement of crystallization rate can be explained by the higher mobility of the branched chains due to a low steric hindrance at the branch point compared to the other branching agents.

Ozawa model

Ozawa considered the nonisothermal crystallization process to be a result of infinitesimal small isothermal crystallization step[29]. The process is rate-dependant and can be written as a function of ϕ, the cooling rate, according to Eq. (13).

$$1-X(T)=\exp\left(-\frac{K(T)}{\phi^m}\right) \tag{13}$$

where $K(T)$ is the cooling function and m the Ozawa exponent, dependent of the crystal growth and nucleation mechanism. The double logarithm plot of lg[−ln(1−$X(T)$)] versus lgϕ for PBS and PBS branched with glycerol propoxylate are given in Fig. 10. If the Ozawa model fits the experiment, the plots at the several temperatures should be linear and parallel among them. As shown in Fig. 10, the plots of neat PBS are parallel unlike the sample with glycerol propoxylate, where m varies according to temperature. Ozawa equation fails to describe the branched samples while it could describe the neat PBS crystallization. This probably results from the Ozawa model that ignores the secondary crystallization. This secondary crystallization has already been highlighted with the Avrami model.

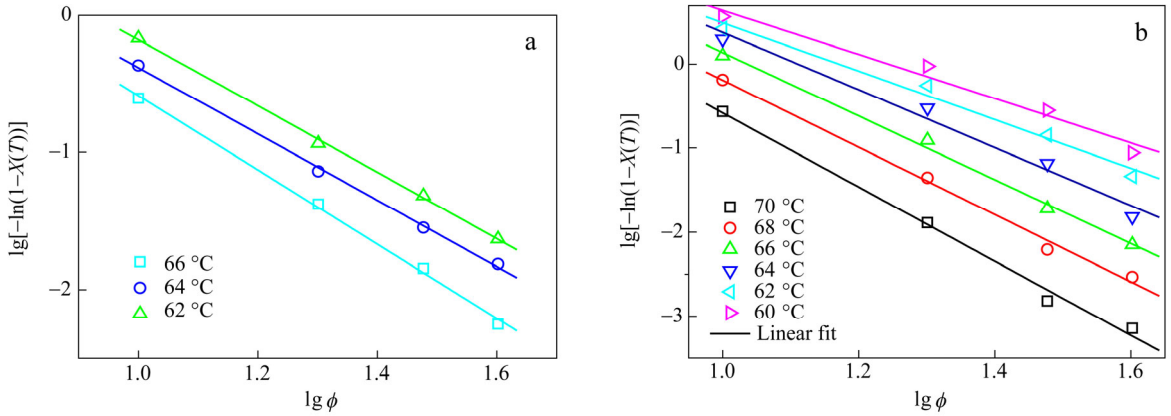

Fig. 10 Ozawa plots of (a) PBS and (b) branched PBS with glycerol propoxylate during the non-isothermal crystallization

Rheological Properties

Rheological measurements were carried out to evaluate the viscoelastic properties of the synthesized polymers. Figure 11 summarizes the complex viscosity of branched samples compared to neat PBS. Linear PBS showed a Newtonian behavior over a large frequency domain (from 0.05 rad/s to 10 rad/s). Branched PBS showed a more obvious shear thinning behavior due to the enlargement of the relaxation spectrum in connection with the delayed reptation of branched chains after completion of the arm retraction under shear. The values of complex viscosity at low frequencies were significantly higher for all branched polymers and could be ranked in the order: PBS < PBS-citric acid < PBS-glycerol propoxylate ≈ PBS-trimesic acid < PBS-TMP. This order can be ascribed to M_w values given in Table 2, respectively 108100, 148400, 153200, 166700, 174500 g/mol.

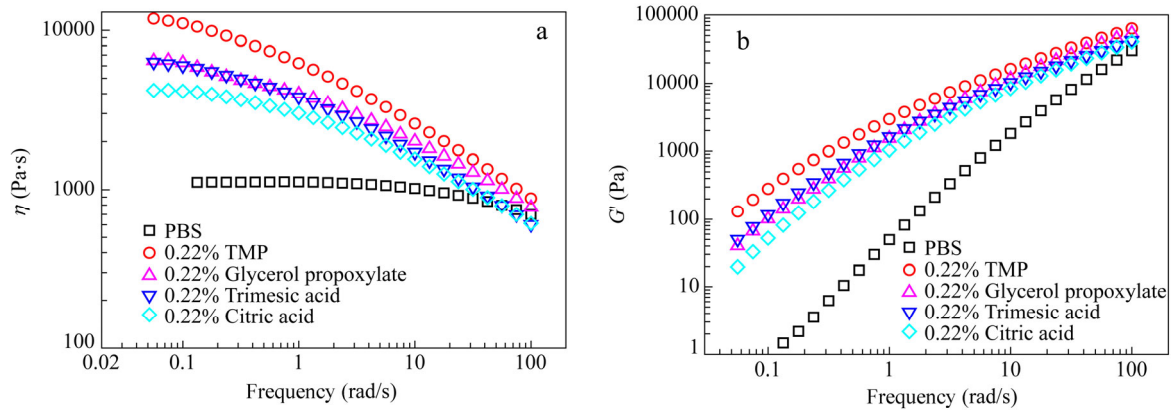

Fig. 11 Dynamic complex viscosity (a), storage modulus (b) as a function of frequency of linear and branched PBS at 130 °C

Both values of G' and G'' were above neat PBS and particularly at low frequencies. This deviation at low frequencies is originated from the long chain branches that relax over longer time and prevent the fast relaxation of the chain backbone. This results in higher elasticity for branched PBS attributed to more entanglements and their persistence at long time scale due to the presence of long chain branching.

With increasing TMP contents from 0.11% to 0.22% in PBS, one can notice an increase in G' at low frequencies whereas at high frequencies it converges with PBS (Fig. 12). Branching shifts the terminal region to lower frequencies, indicating a much longer time to get the molecule fully relaxed. A linear polymer chain relaxes by reptation, however, in branched chains, this reptation is hindered by the branch points. The arms must retract at shorter time before reptation of the main backbone can take place at longer time. The relaxation hence occurs from the outside of the polymer chain towards the inside. Nevertheless the behavior of 0.5% TMP is unexpected and difficult to interpret in this frame. A plausible explanation may be a degradation of this sample but also an increase of the steric hindrance between branches at strong branching degree as confirmed by the spectacular decrease of the modulus at high frequencies in the vicinity of the entangled plateau region.

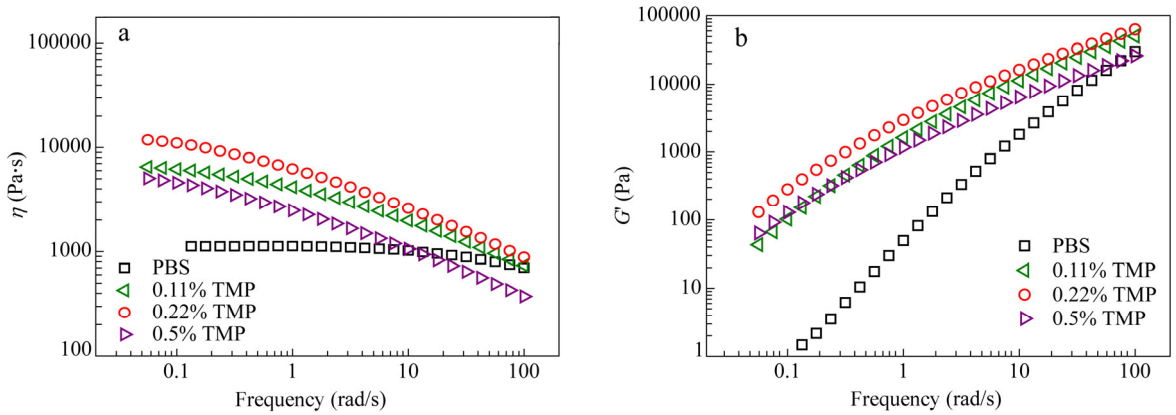

Fig. 12 Dynamic complex viscosity (a), storage modulus (b) as a function of frequency of linear and branched PBS with TMP at 130 °C

Relaxation spectra analysis

To compare the relaxation behavior of branched PBS, the weight relaxation spectra were calculated according to Eq. (14).

$$G^{\rightarrow}(\omega,\lambda)=\int_{-\infty}^{+\infty}\frac{H(\lambda)i\omega\lambda}{\lambda(1+i\omega\lambda)}\mathrm{d}\lambda \tag{14}$$

ω is the frequency and λ is the relaxation time.

The weight relaxation spectra $H(\lambda)\lambda$ are presented in Fig. 13. These spectra reveal the relaxation time distribution which is related to the relaxation of different kinds of chains at various processes. For branched polymers with TMP, trimesic acid and glycerol propoxylate bimodal distributions are observed. This double time relaxation distribution was observed for branched PE and branched PP[30, 31]. The first peak appears at relaxation time close to linear PBS and the second one at higher relaxation time. This means that two relaxation processes occur. The first relaxation is attributed to the reptation of linear chains. The second relaxation time is attributed to the relaxation of long branched chains which mobility is restricted due to the presence of branch point. For citric acid branched polymers, the second relaxation is less marked.

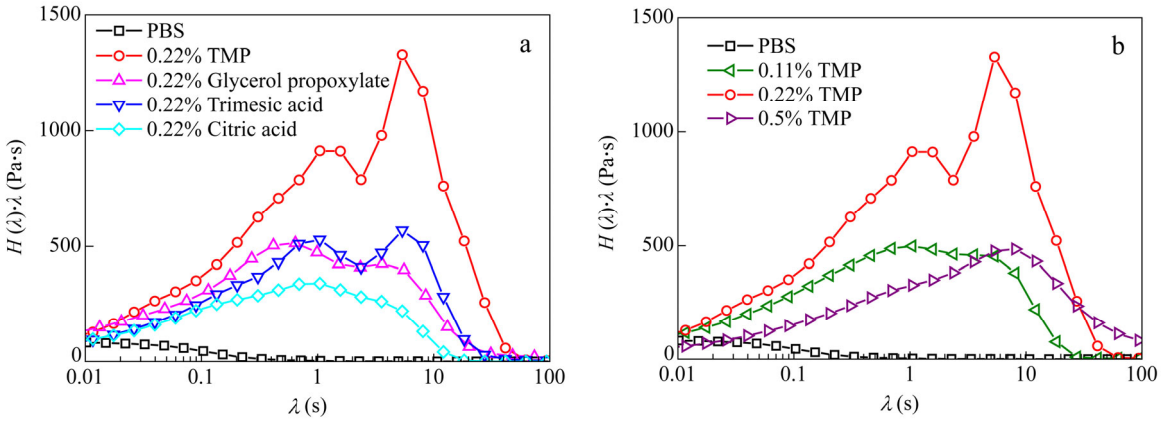

Fig. 13 Weighed relaxation spectra of (a) branched PBS with various branching agents at 0.22% (b) branched PBS with TMP

Topology determination using van-Gurp-Palmen plots

Recent publications proposed a convenient and reliable tool to characterize branched polymer melts and to determine their topology using the reduced van-Gurp-Palmen plot (rvGP)[32, 33]. These authors studied polymers with different topologies and highlighted the existence of fingerprints. Rheological data are shown by plotting the phase angle δ versus G_{red} which is the complex modulus normalized to plateau modulus as defined by both Eqs. (15) and (16).

$$G_{red} = \frac{\left|G^{\rightarrow}\right|}{G_N^0} \tag{15}$$

$$G_N^0 = \lim_{\delta \to 0} \left|G^{\rightarrow}(\delta)\right| \tag{16}$$

One tremendous advantage of this representation is that the chemical composition or copolymer composition do not influence the curve anymore and allow to compare polymers of different chemical structures[33]. While molar mass does not influence the shape of the curve, dispersity tends to stretch the curve. This approach has already been used to determine the topology of branched PLA[34].

The linear samples show the characteristic curve of a linear polymer with a curve reaching the phase angle of 90° at low reduced moduli G_{red}[32]. Branched samples all show a different curvature compared to the neat PBS (Fig.14).

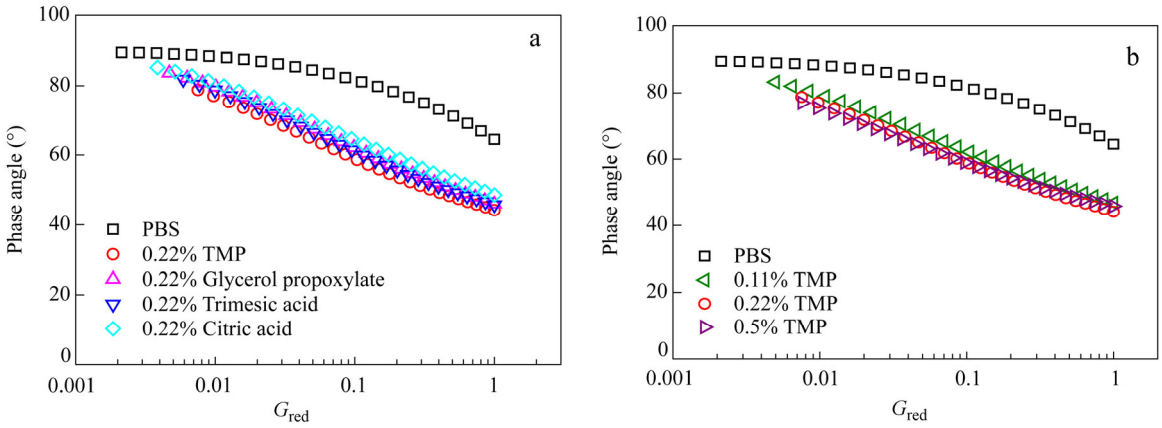

Fig. 14 Reduced van-Gurp-Palmen plots of (a) branched PBS with various branching agents at 0.22% and (b) branched PBS with TMP

It was already proven that by adding long chain branching rvGP plots shifted to lower phase angle[35]. This behavior is marked when branching agent content increases from 0.11% to 0.22%. This corroborates their stronger elasticity. At 0.5% of TMP a slight bump is observed at high G_{red} assessing that a change in topology is created. According to the studies of Lohse *et al.*[35] for well defined structures, and in accordance with the number of branch points by chain, some small branches may appear with 0.5% TMP while with 0.22% TMP three arm structures are probably obtained. Although trends can be postulated, the exact topology is not known since rvGP plot of the branched polymers does not really match with a polymer with known topology (three-arm or four-arm star polymer, H-shaped polymer). It is believed to be a statistical mixture of linear and branched polymers with different topologies. The number of branches per chain calculated was inferior to 1 for 0.22% of branching agent and confirms the presence of linear and branched chains.

Mechanical Properties of Films Prepared by Extrusion Blowing

A series of materials have been synthesized with 200 mg of Ti per kg of PBS polymer in order to blow and test films. The introduction of branches improves melt strength and greatly facilitates the extrusion blowing of the material that was relatively easy to process and comparable to films of polyethylene.

The mechanical properties of films have been measured on normalized dogbone specimens cut along both longitudinal and transversal directions relative to the direction of extrusion (Table. 4). The addition of branching agent increases significantly the modulus and the stress at break of polymer films. For instance the modulus of PBS containing 0.5 mol% TMP increased largely. As a consequence of this increase of modulus, the introduction of branching agents tends to promote a premature rupture of the sample, and thus causes a decrease of the elongation at break. By comparing the polymer properties on both stretching directions, it appears that for the highest branching agent contents, film properties vary with the film orientation. In fact it appears that these films are able to be elongated only in the longitudinal direction. This is more noticeable for PBS prepared with TMP, trimesic acid or glycerol propoxylate. In these cases we suspect the formation of an oriented structure during the film processing which leads to the obtaining of a non-isotropic material.

Table 4. Mechanical properties of branched PBS films

Branching agent	Branching ratio in polymer [a] (mol%)	Film χ_c (%)	Modulus (MPa)		Stress at break (MPa)		Elongation at break (%)	
			Long.	Trans.	Long.	Trans.	Long.	Trans.
PBS	0	32	150	150	19	17	230	170
Malic acid	0.03	34	160	140	23	17	100	250
	0.08	34	210	210	29	32	50	40
	0.12	34	190	210	28	38	40	30
	0.30	28	220	320	39	43	50	20
Trimethylolpropane	0.20	33	200	260	37	30	130	10
	0.50	30	270	400	37	30	135	10
Trimesic acid	0.21	30	210	280	33	28	360	30
Glycerol propoxylate	0.21	31	210	230	41	23	310	30

[a] Evaluated by using ^{1}H-NMR spectroscopy

CONCLUSIONS

Branched PBS were successfully synthesized by using multifunctionnal comonomers directly introduced in the feed with 1,4 butanediol and succinic acid. The polymer characteristics were determined by using SEC and ^{1}H-NMR and confirmed the introduction of the branching agents. The samples got between 0.28 and 0.89 branch points per chain. Among the branching agents tested, glycerol propoxylate offered improved crystallization properties with an increase of the crystallization rate in both isothermal and non-isothermal conditions. This feature was attributed to the higher mobility of the branching agents compared to others like TMP, citric acid or trimesic acid. A secondary nucleation was observed with glycerol propoxylate attributed to the crystallization of amorphous fraction included between crystallites formed at the primary crystallization.

Linear rheology in oscillatory shear suggested that branching occurred with all branching agents. Typical features such as high elasticity and complex viscosity at low frequencies or marked shear thinning behavior were observed. The bimodal relaxation spectra confirmed the presence of linear chains coupled with branched chains that relaxed over longer time and induced broadening of the spectrum. Topology of the structure obtained was also determined using reduced van-Gurp-Palmen plots. The plots revealed characteristics curves of a combination between linear and long-chain branched chains. It follows that branched PBS was more easily processed by film blowing. The results of tensile testing showed that branched structures increased the modulus and the stress at break of polymer films.

REFERENCES

1 Jacquel, N., Saint-Loup, R., Pascault, J.P., Rousseau, A. and Fenouillot, F., Macromol. Mater. Eng., 2014, 299(8): 977
2 Takashi, F., Polym. Degrad. Stab., 1998, 59(1–3): 209
3 Han, Y.K., Kim, S.R. and Kim, J., Macromol. Research, 2002, 10(2): 108
4 Kim, E.K., Bae, J.S., Im, S.S., Kim, B.C. and Han, Y.K., J. Appl. Polym. Sci., 2001, 80(9): 1388
5 Wang, G., Guo, B. and Li, R., J. Appl. Polym. Sci., 2012, 124(2): 1271
6 Garin, M., "Synthèse et étude des propriétés physico-chimiques des poly(butylène succinate)s linéaire et branché.", Thesis, University of Reims Champagne-Ardenne, 2012
7 Han, Y.K., Um, J.W., Im, S.S. and Kim, B.C., J. Polym. Sci., Part A: Polym. Chem., 2001, 39(13): 2143
8 Nagata, M., Kiyotsukuri, T., Hasegawa, T., Tsutsumi, N. and Sakai, W., J. Macromol. Sci., Part A, 1997, 34(6): 965
9 Jin, H.J., Kim, D.S., Lee, B.Y., Kim, M.N., Lee, I.M., Lee, H.S. and Yoon, J.S., J. Polym. Sci., Part B: Polym. Phys., 2000, 38(17): 2240
10 Teramoto, N., Ozeki, M., Fujiwara, I. and Shibata, M., J. Appl. Polym. Sci., 2005, 95(6): 1473
11 Suhartini, M., Mitomo, H., Nagasawa, N., Yoshii, F. and Kume, T., J. Appl. Polym. Sci., 2003, 88(9): 2238
12 Zhou, H., Wang, X., Du, Z., Li, H. and Yu, K., Polym. Eng. Sci., 2014, 55: 988
13 Wang, G., Gao, B., Ye, H., Xu, J. and Guo, B., J. Appl. Polym. Sci., 2010, 117(5): 2538
14 Jin, H.J., Park, J.K., Park, K.H., Kim, M.N. and Yoon, J.S., J. Appl. Polym. Sci., 2000, 77(3): 547
15 McKee, M.G., Unal, S., Wilkes, G.L. and Long, T.E., Prog. Polym. Sci., 2005, 30(5): 507
16 Jacquel, N., Freyermouth, F., Fenouillot, F., Rousseau, A., Pascault, J.P., Fuertes, P. and Saint-Loup, R., J. Polym. Sci., Part A: Polym. Chem., 2011, 49(24): 5301
17 Papageorgiou, G.Z. and Bikiaris, D.N., Polymer, 2005, 46(26): 12081
18 Fujihira, R., Fujimaki, T., Ichikawa, Y., Imaizumi, M., Kimura, H., Moteki, Y., Suzuki, J. and Takiyama, E., 2004, E.P. Pat., 0747416 B1
19 Aoshima, T., Miki, Y., Kumazawa, K., Katou, S., Uyeda, T., Hoshino, T., Shintani, N., Yamagishi, K. and Isotani, A., 2011, U.S. Pat., 7985566 B2
20 Hoshino, T., Matsuzono, S., Kaneko, H., Hamano, T., Aoshima, T. and Ueda, T., 2012, U.S. Pat., 8318893 B2
21 Charlier, Q., Girard, E., Freyermouth, F., Vandesteene, M., Jacquel, N., Lavadière, C., Rousseau, A. and Fenouillot, F., eXPRESS Polym. Lett., 2015, 9(5): 424
22 Jin, T.X., Zhou, M., Hu, S.D, Chen, F., Fu, Q. and Fu, Y., Chinese J. Polym. Sci., 2014, 32(7): 953
23 Ichikawa, Y., Mizukoshi, T., "Synthetic biodegradable polymers", ed. Rieger, B., Künkel, A., Coates, G.W., Reichardt, R., Dinjus, E. and Zevaco, Th.A., Springer, 2012, p.285
24 Avrami, M., J. Chem. Phys., 1939, 7(12): 1103
25 Avrami, M., J. Chem. Phys., 1940, 8(2): 212
26 Papageorgiou, G.Z., Achilias, D.S. and Bikiaris, D.N., Macromol. Chem. Phys., 2009, 210(1): 90
27 Li, Y.D., Zeng, J.B., Li, W.D., Yang, K.K., Wang, X.L. and Wang, Y.Z., Industrial & Engineering Chemistry Research, 2009, 48(10): 4817
28 Jeziorny, A., Polymer, 1978, 19(10): 1142

29 Ozawa, T., Polymer, 1971, 12(3): 150
30 Wood-Adams, P. and Costeux, S., Macromolecules, 2001, 34(18): 6281
31 Zhao, W., Huang, Y., Liao, X. and Yang, Q., Polymer, 2013, 54(4): 1455
32 Trinkle, S. and Friedrich, C., Rheologica Acta, 2001, 40(4): 322
33 Trinkle, S., Walter, P. and Friedrich, C., Rheologica Acta, 2002, 41(1–2): 103
34 Liu, J., Lou, L., Yu, W., Liao, R., Li, R. and Zhou, C., Polymer, 2010, 51(22): 5186
35 Lohse, D.J., Milner, S.T., Fetters, L.J., Xenidou, M., Hadjichristidis, N., Mendelson, R.A., García-Franco, C.A. and Lyon, M.K., Macromolecules, 2002, 35(8): 3066